Architecture, process, and materials for efficient inorganic-organic hybrid solar cells

April 13, 2015

Sang Il Seok

- ❖ **Center for Solar Energy Materials Research, Korea Research Institute of Chemical Technology, Korea (seoksi@krict.re.kr)**
- ❖ **Future Solar cells Lab., Department of Energy Science, Sungkyunkwan University, Korea. (seoksi@skku.edu)**

KRICT Korea Research Institute of Chemical Technology

Global Solar Market Outlook

- **2013 Total Installation**: **37 GW**
  - 11.3GW/China, 10.3GW/EU, 7.5GW/Japan, 4.8GW/USA, 4.1GW/ROW
- **2014 Global Demand Forecast** : **47GW**
  - 14GW/China, 10GW/ EU (3GW/UK, 2.5GW/Germany..), 8GW/Japan, 7GW/USA, 8GW/ROW (India, MEA, South America, South Africa, ..)
  - Supply capacity~63GW; effective capacity~45GW
  - Transition to supply-driven market in 2014

~60GW in 2015

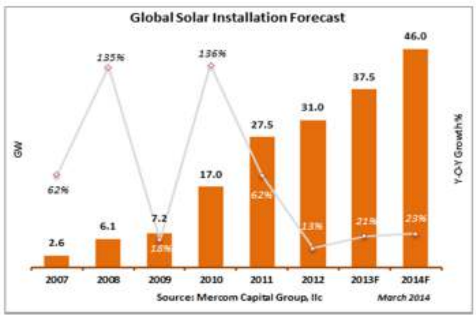

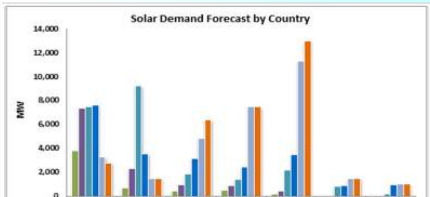

	Germany	Italy	US	Japan	China	UK	India
2009	3,806	711	477	484	160	10	6
2010	7,400	2,321	961	893	433	62	12
2011	7,487	9,248	1,855	1,404	2,200	813	172
2012	7,603	3,577	3,192	2,467	3,500	925	986
2013F	3,304	1,500	4,840	7,505	11,300	1,500	1,004
2014F	2,750	1,500	6,400	7,500	13,000	1,500	1,000

Sources: RPIA (European PV industry association)

KRICT Korea Research Institute of Chemical Technology

KRICT hybrid solar cells

Adv. Mater. 26, 1622–1628 (2014)

Cell type (area if <1 cm^2)	Best lab. cell efficiency, η_{LC} [%] (in 2011)
sc-Si	25.0
mc-Si	20.4
CIGS	[a]19.6
a-Si	10.1
CdTe	19.6 (16.7)
GaAs	28.8 (28.1)
GaInP (0.25)	20.8 (17.4)
DSSC	12.3 (11.1)[b]
OPV (thinfilm)	10.7 (8.3)[a]
CZTSS (0.45)	11.1 (9.7)
CZTS (0.45)	8.4
Perovskite $CH_3NH_3PbI_3$ (0.28)	15 (6.5)[b] → >20%
Perovskite $CH_3NH_3PbI_{3-x}Cl_x$ (0.08)	15.4[b]
PbS-CQD (0.05)	7 (4.4)[b]
Sb_2S_3(ETA) (0.16)	6.3 (5.1)[b] → > 8%

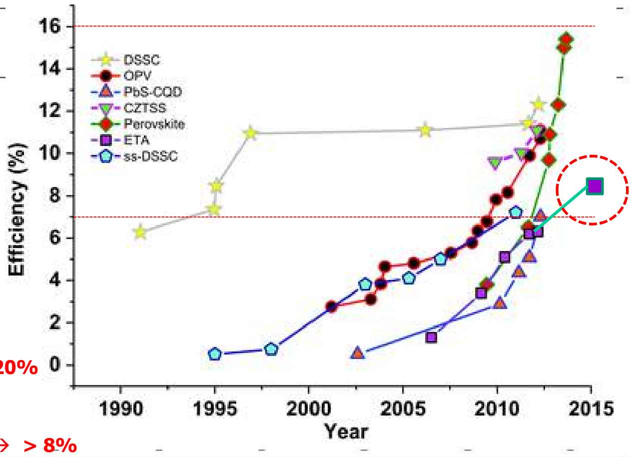

[a]Higher efficiencies that have been reported for cells with <1 cm^2 area are (in %) as follows: CIGS (20.4),[52] OPV (11.1)[52]; [b]Efficiency values of DSSC, for the perovskites $CH_3NH_3PbI_3$, $CH_3NH_3PbI_{3-x}Cl_x$, and for PbS- CQD and Sb_2S_3 (ETA) cells are from refs.[15,43,44,47] and,[53] respectively; [c]Calculated from the total area of the module; [d]Values are from Nayak et al;[6] [e]Added during proof stage CIGS: $Cu(In_{\sim 0.7}Ga_{\sim 0.3})Se$; CZTSS: $Cu_2ZnSn(S,Se)_4$; CZTS: $Cu_2ZnSn(S)_4$; OPV: Organic photovoltaic (cell); PbS-CQD: PbS colloidal quantum dot; ETA: extremely thin absorber.

KRICT Korea Research Institute of Chemical Technology 3

KRICT hybrid solar cells

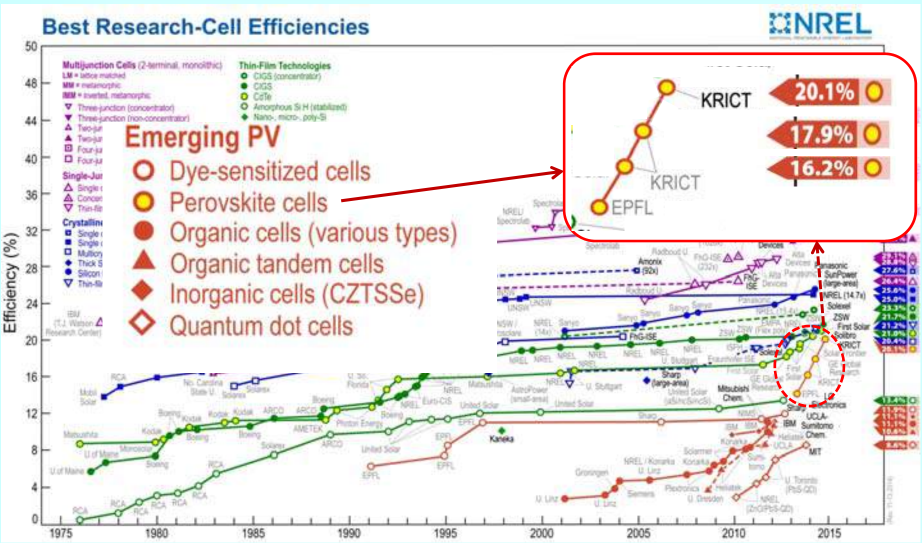

KRICT Korea Research Institute of Chemical Technology 4

Outline

- State-of-art of solar cells
- Research scheme: Why inorganic-organic heterojunction hybrid solar cells?
- Inorganic-organic hybrid solar cells

✓ $Sb_2S(e)_3$-based systems

✓ $APbX_3$ perovskite-based systems

➢ A $=CH_3NH_3$, $HN=CHNH_2$; x=I, Br. Cl

- Summary

State-of-the- Art of Solar cells

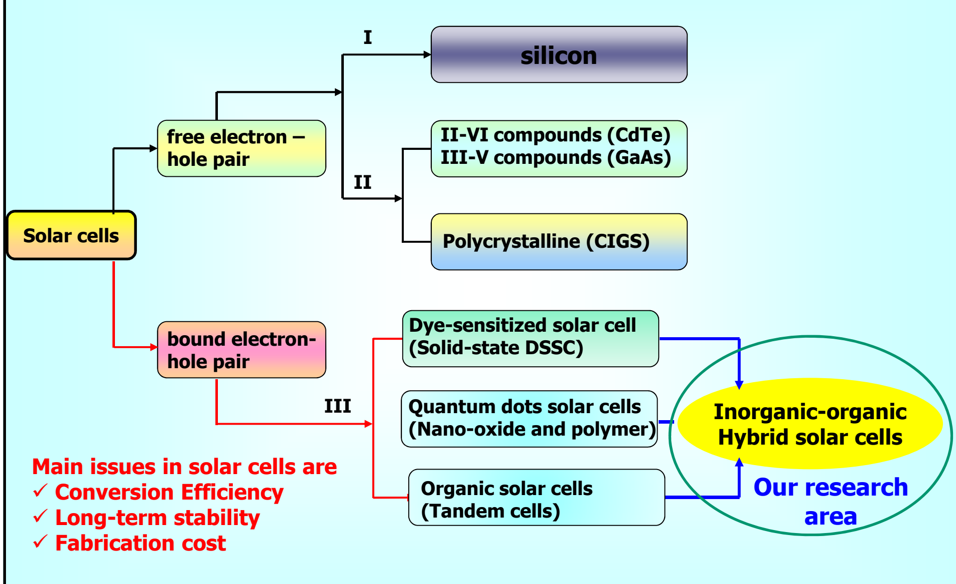

Inorganic-organic hybrid solar cells

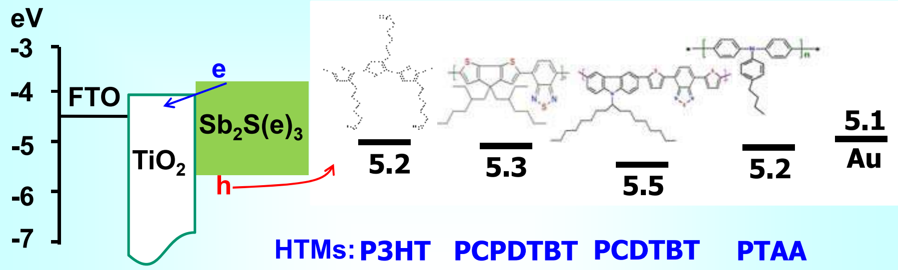

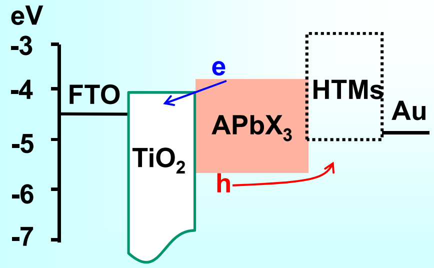

P3HT: poly(3-hexylthiophene)
PCPDTBT: poly(2,6-(4,4-bis-(2-ethylhexyl)-4*H*-cyclopenta[2,1-*b*;3,4-*b*′]dithiophene)-alt-4,7(2,1,3-benzothiadiazole)
PCPTBT: poly (*N*-9′′-heptadecanyl-2,7-carbazole-alt-5,5-(4′,7′-di-2-thienyl-2′,1′,3′-benzothiadiazole)
PTAA: poly(triarylamine)

Sb-CHs-based inorganic-organic hybrid solar cells

Architecture

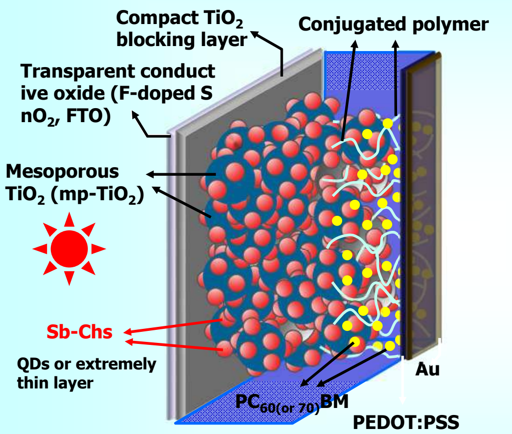

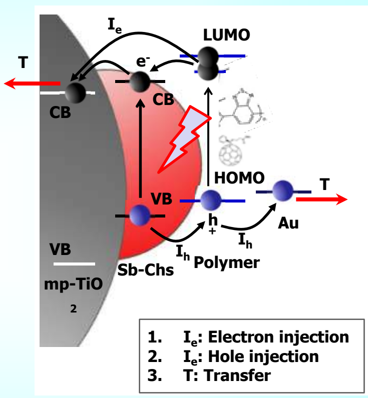

- $PC_{60}BM$ / phenyl-C60-butyric acid methyl ester
- PEDOT:PSS / poly(3.4-ethylenedioxythiophene) poly(styrenesulfonate)

Nanostructured Sb_2S_3/P3HT heterojunction solar cells

Sb_2S_3: a high absorption coefficient (1.8 × 10^5 cm^{-1} at 450 nm) and optimum bandgap (E_g = 1.7 eV)

Precursors: $SbCl_3$ and Sodium thiosulfate

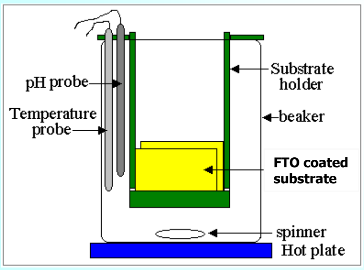

CBD Process

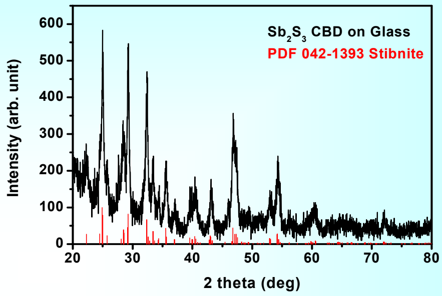

XRD pattern of Sb_2S_3 annealed at ~300 °C after CBD

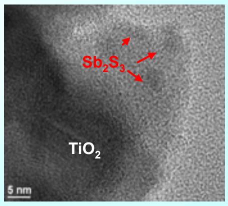

KRICT Korea Research Institute of Chemical Technology

mp-TiO_2/Sb_2S_3/P3HT hybrid solar cells

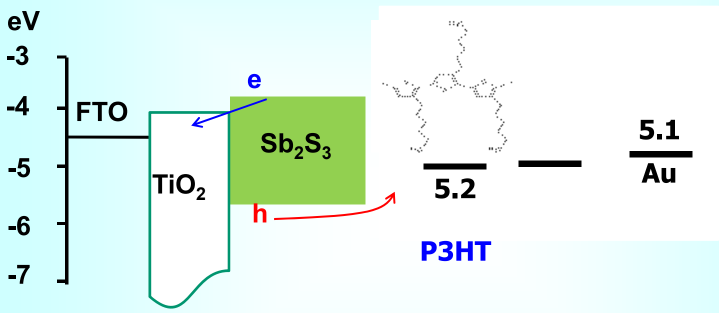

P3HT: poly(3-hexylthiophene)

KRICT Korea Research Institute of Chemical Technology

Nanostructured Sb_2S_3/P3HT heterojunction solar cells

Current density-voltage (*J-V*) curves

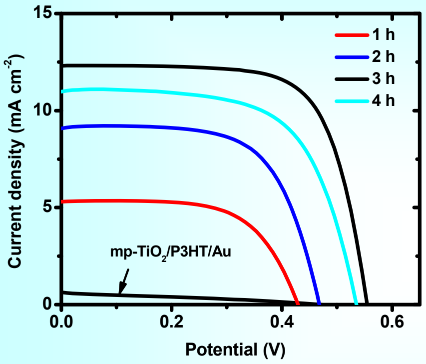

Incident-photon-to-current conversion efficiency (IPCE)

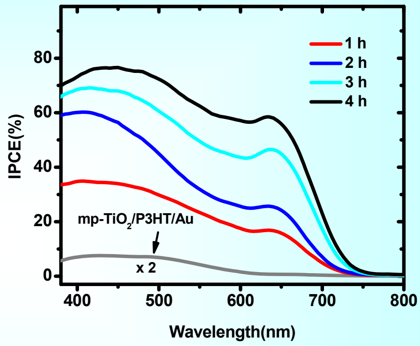

Nano Letters, 10, 2609 (2010)

CBD time (h) for Sb_2S_3	J_{sc}[mA cm^{-2}]	V_{oc}[mV]	*FF*[%]	*Eff.*[%]
0	0.63	475	29.2	0.092
1	5.3	424	64.1	1.48
2	9.1	465	65.5	2.92
3	12.3	556	69.9	5.06
4	11.0	535	63.8	3.97

Nanostructured Sb_2S_3/P3HT heterojunction solar cells

Stability with time

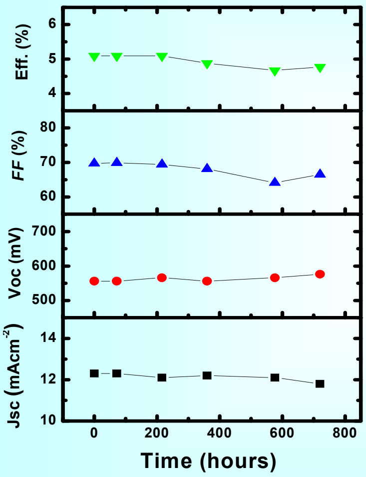

Reproducibility: OK !

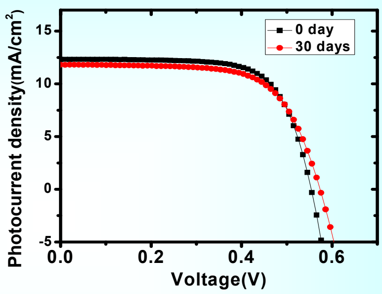

Time [hours]	Jsc [mA/ cm²]	Voc [mV]	*Ff* [%]	*Eff.* [%]
0	12.3	556	69.7	5.09
72	12.3	556	69.9	5.09
216	12.1	566	69.4	5.09
360	12.2	556	68.1	4.88
576	12.1	566	64.1	4.66
720	11.8	576	66.5	4.77

Inorganic-organic hybrid solar cells

mp-TiO_2/Sb_2S_3/HTMs

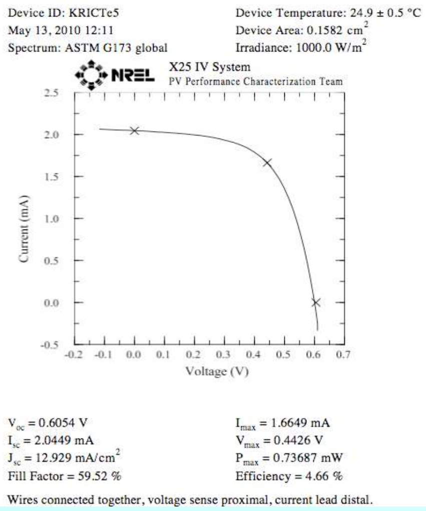

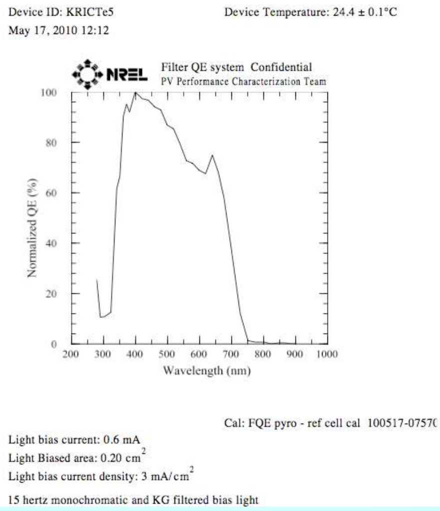

KRICT Korea Research Institute of Chemical Technology 13

Nanostructured Sb_2S_3/various CPs heterojunction solar cells

Optical and electrical properties of P3HT, PCPDTBT, PCDTBT, and PTAA

Conducting polymers	Band gap(eV)	LUMO (eV)	HOMO (eV)	Hole mobility ($cm^2V^{-1}s^{-1}$)
P3HT	2.0	-3.2	-5.2	4.0×10^{-4} (a)
PCPDTBT	1.45	-3.55	-5.3	4.5×10^{-4} (a)
PCDTBT	1.9	-3.6	-5.5	1.0×10^{-4} (a)
PTAA	3.0	-2.2	-5.2	$\sim 4 \times 10^{-3}$ (b)

a: Space charge limited current (SCLC) hole mobility
b: Hole mobility from field effect transistor

P3HT: poly(3-hexylthiophene)
PCPDTBT: poly(2,6-(4,4-bis-(2-ethylhexyl)-4*H*-cyclopenta[2,1-*b*;3,4-*b*′]dithiophene)-alt-4,7(2,1,3-benzothiadiazole)
PCPTBT: poly (*N*-9′′-heptadecanyl-2,7-carbazole-alt-5,5-(4′,7′-di-2-thienyl-2′,1′,3′-benzothiadiazole)
PTAA: poly(triarylamine)

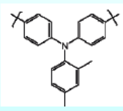

J. AM. CHEM. SOC. 2009, *131*, 10814–10815

KRICT Korea Research Institute of Chemical Technology 14

Nanostructured Sb_2S_3/various CPs heterojunction solar cells

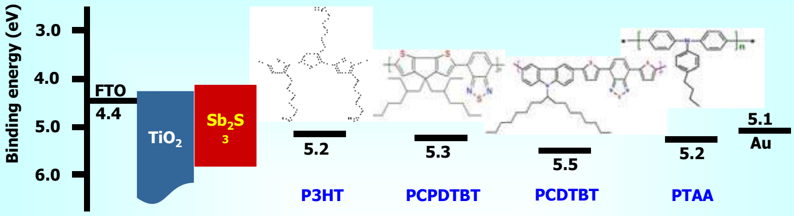

$$\eta = \frac{P_{max}}{E \cdot A_c} = \frac{FF \cdot I \cdot V}{E \cdot A_c}$$

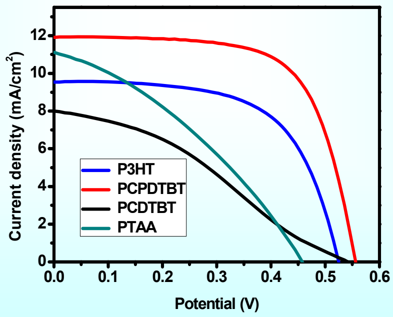

Efficient hole extraction

Toward bi-thiophene moiety in a CP

Speculation: Bi-thiophen break the long Sb-S bond and form bidentate chelating bond to Sb

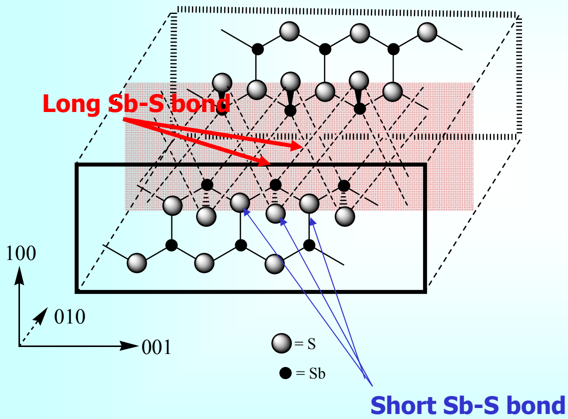

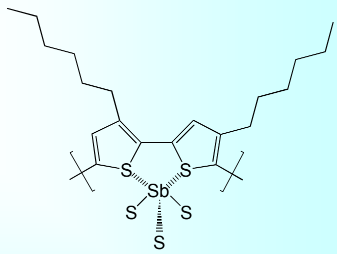

Nano Lett. 2011, 11, 4789–4793

Efficient hole extraction

Toward bi-thiophene moiety in a CP

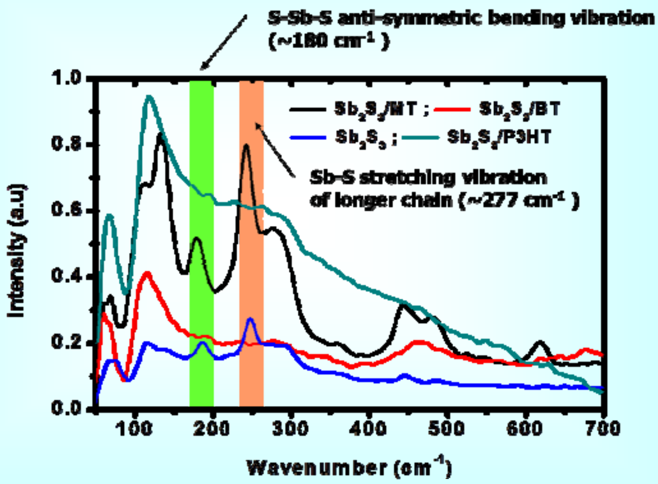

Nano Lett. 2011, 11, 4789–4793

Sb_2S_3/PCPDTBT heterojunction solar cells

***J-V* curves over a range of intensities**

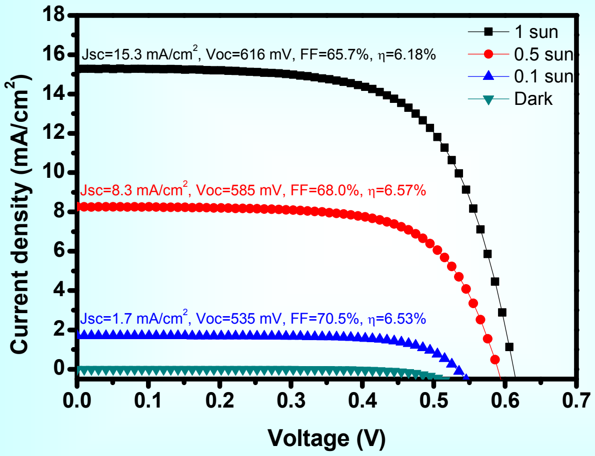

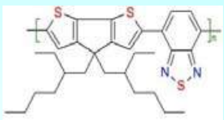

PCPDTBT

Nano Lett. 2011, 11, 4789–4793

Nanostructured Sb_2S_3/P3HT heterojunction solar cells

- UV-visible absorption spectra
- (wavelength of excitation light = 530 nm)

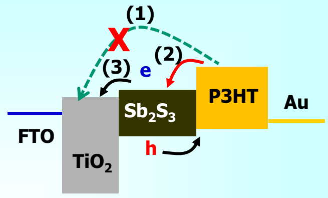

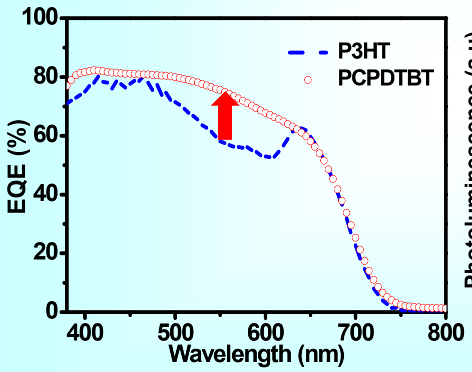

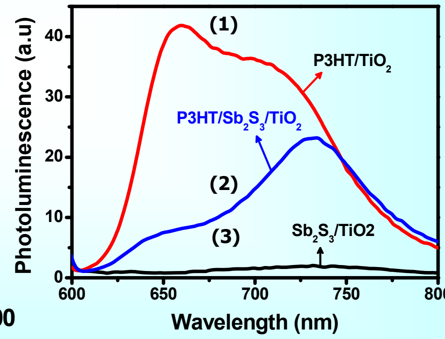

Nanostructured Sb_2S_3/P3HT(PCBM) heterojunction solar cells

Panchromatic Photon-Harvesting by Hole-Conducting Materials

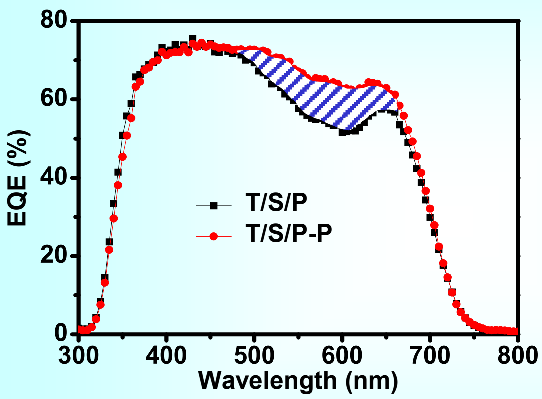

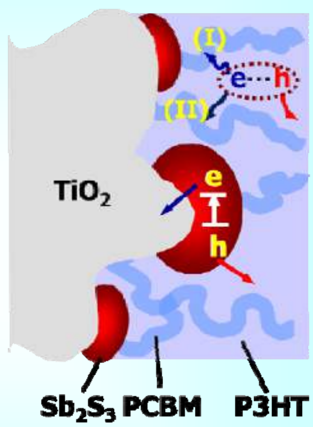

PCBM : [6,6]-phenyl-C_{61}-butyric acid methyl ester

Nanostructured Sb_2S_3/PCPDTBT(PCBM) heterojunction solar cells

Panchromatic Photon-Harvesting by Hole-Conducting Materials

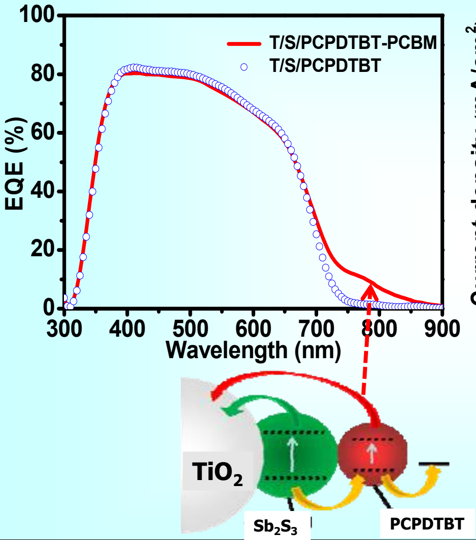

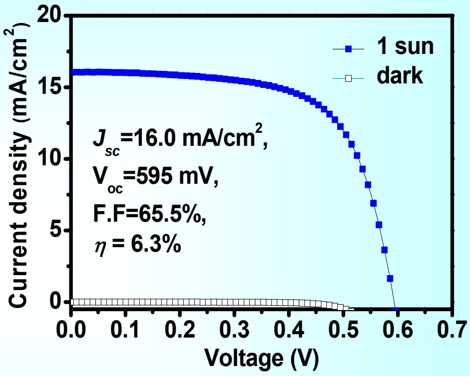

Nano Lett. 12, 1863 (2012)

Sb_2S_3-based inorganic-organic hybrid solar cells

Passivation after CDD

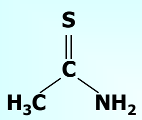

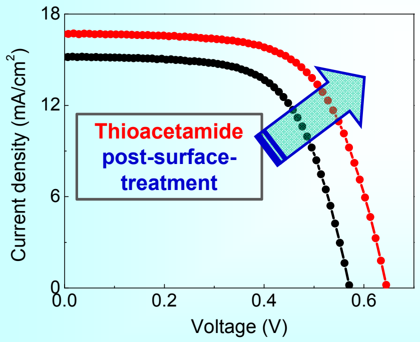

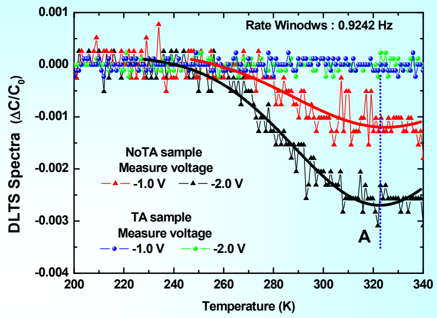

Champion device

Light power (mW cm^{-2})	J_{SC} (mA cm^{-2})	V_{OC} (mV)	FF (%)	PCE (%)
100	16.1	711.0	65.0	7.5
50	9.6	672.7	67.0	8.7
10	2.0	600.1	70.0	8.4

Adv. Func. Mater. 24, 3587 (2014)

mp-TiO_2/$CuSb_2S_2$/PCPDTBT hybrid solar cells

Process

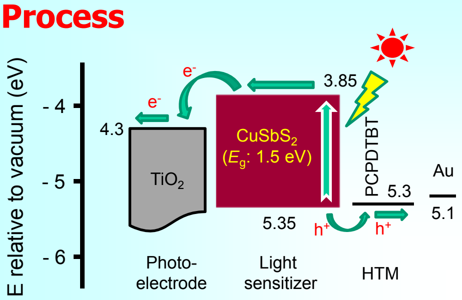

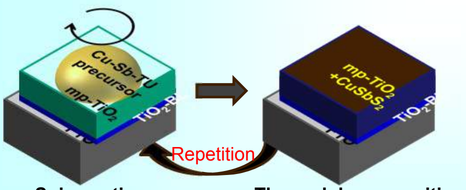

Cu-Sb-TU complex sol

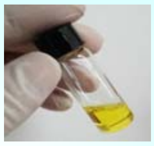

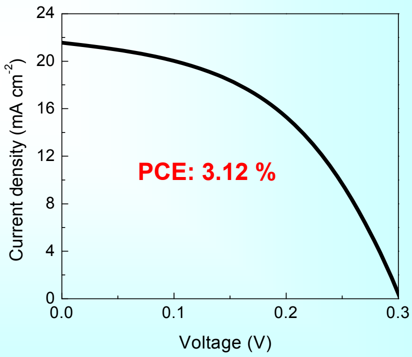

Angew. Chem. Int. Ed. 54, 4005 (2015)

Perovskite fever

Staggering increases in the performance of organic-inorganic perovskite solar cells have renewed the interest in these materials. However, further developments and the support from academic and industrial partners will hinge on the reporting of accurate efficiency values.

Nature Materials 13, 837 (2014) doi:10.1038/nmat4079
Published online 21 August 2014

What is Perovskite?

Most widely studied oxide structure: ABO_3

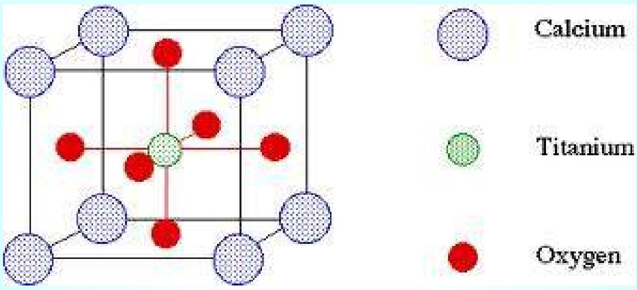

- **A perovskite structure is any material with the same type of crystal structure as calcium titanium oxide ($CaTiO_3$), known as the perovskite structure ABO_3.**
- **Named after Russian mineralogist L. A. Perovski.**

Hybrid Perovskites

Perovskite structure=AMX_3

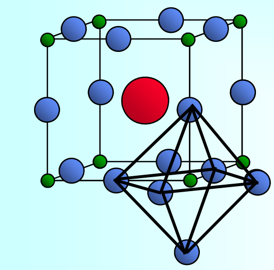

A-cation 12-fold coordinated
M-cation, octahedrally coord.
X-Halide

Schematic of MX_6 octahedra and the organic moiety of the basic AMX_3 perovskite unit cell and three-dimensional network formed by AMX_3 perovskite unit cells.

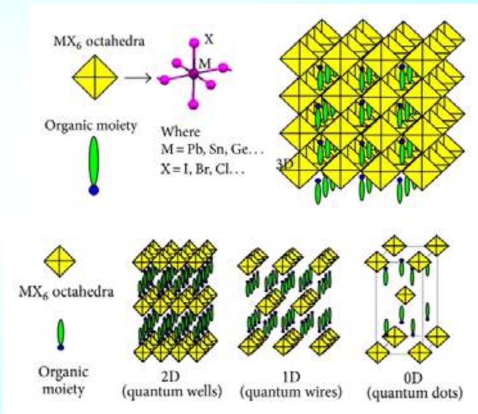

Schematic of 2D, 1D, and 0D IO-hybrid derived from parent AMX_3 type 3D IO-hybrid

J. of Nanoparticles, 2013, 531871 (2013)

Architectures

Perovskite-sensitized solar cells

Replacing Dye with Perovskite: Current Perovskite Solar Cells are built upon the architectural basis for DSSCs pioneered by Grätzel (EPFL, Switzerland)

mp-$CH_3NH_3PbI(Br)_3$/electrolyte ($LiI(Br)/I(Br)_2$ in acetonitrile)

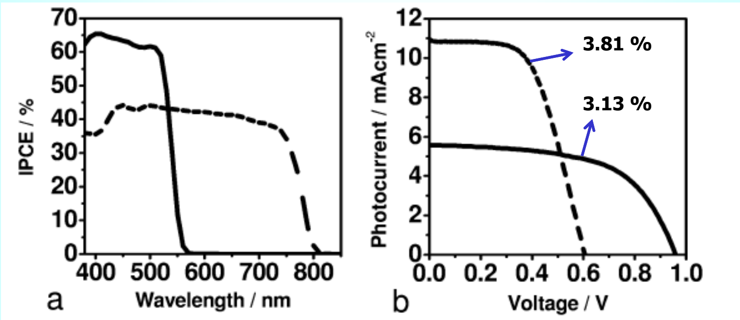

(a) IPCE spectra and (b) I-V action scharacteristic for mp-TiO_2/$CH_3NH_3PbBr_3$ (solid line) and $CH_3NH_3PbI_3$/TiO_2 (dashed line)

→ 6.5 % (N. G. Park et al., Nanoscale, 3, 4088−4093. 2011)

T. Miyasaka et al., J. Am. Chem. Soc. 131, 6050 (2009)

Architectures

Perovskite-sensitized solar cells

Replace Liquid Electrolyte with a Solid Hole Transporting Layer (HTL)

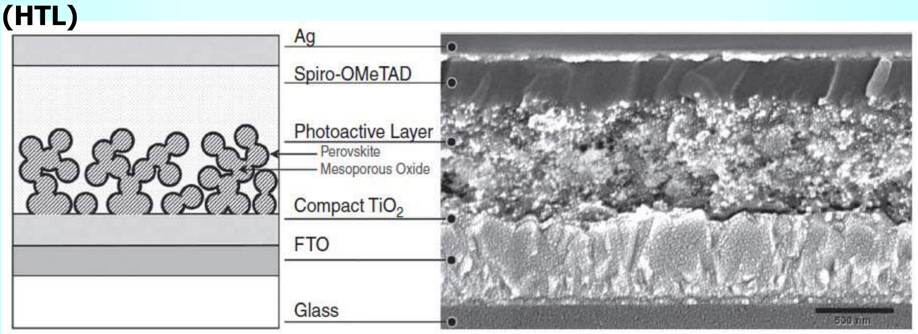

Left: Schematic representation of full device structure, where the mesoporous oxide is either Al_2O_3 or anatase TiO_2. Right: Cross-sectional SEM image of a full device incorporating mesoporous Al_2O_3. Scale bar, 500 nm.

- ✓ The construction of a planar-junction diode with the structure FTO/compact TiO_2/$CH_3NH_3PbI_2Cl$/spiro-OMeTAD/Ag.
- ✓ spiro-OMeTAD: 2,2´,7,7´-tetrakis-(N,Ndi-p-methoxyphenylamine)9,9´-spirobifluorene

H. Snaith et al., Science, 338, 643 (2012)
Received 31 May 2012

Architectures

Perovskite-sensitized solar cells

Replace Liquid Electrolyte with a Solid Hole Transporting Layer (HTL)

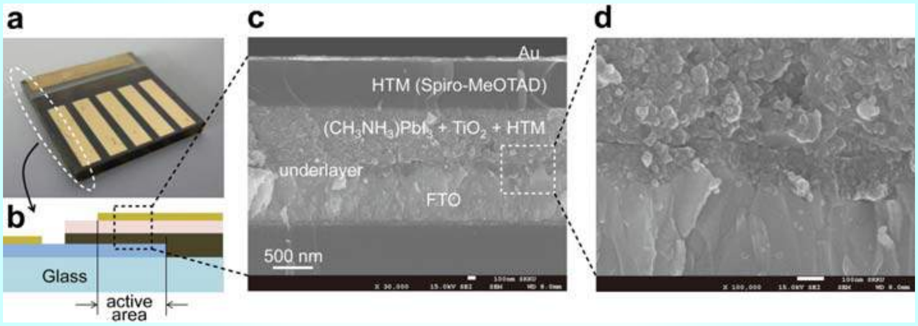

(a) Real solid-state device. (b) Cross-sectional structure of the device. (c) Crosssectional SEM image of the device. (d) Active layer-underlayer-FTO interfacial junction structure

N.G. Park eta al., Sci. Report, 2, 591 (2012)

Received 5 July 2012

Architectures: new era

Inorganic-organic hybrid perovskite solar cells

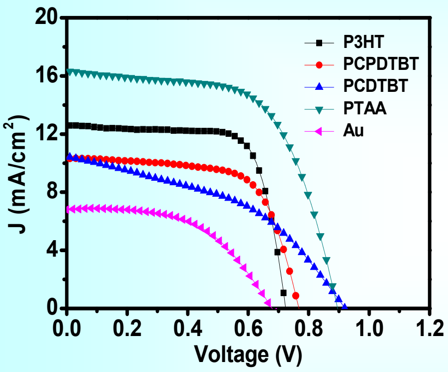

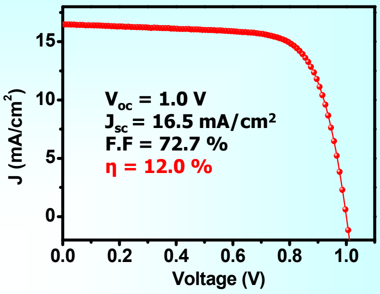

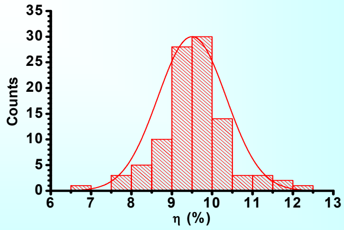

Nature Photonics, 7, 486 (2013)

Architectures

SEM cross-sectional image

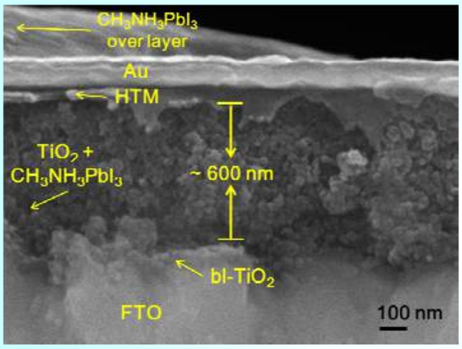

SEM surface image

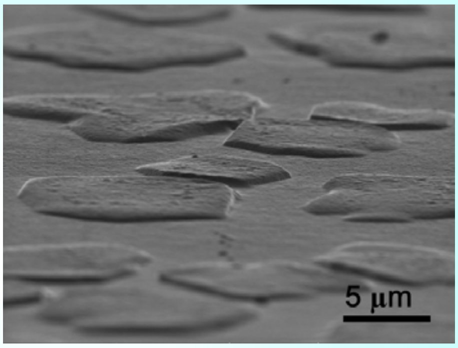

→ **Dense nanocomposite and thin upper layers**
→ **Is different with conventional dye-sensitized structure**
→ **Perovskite $CH_3NH_3PbI_3$ as both light harvester and hole conductor**

Architectures

XPS (X-ray photoelectron spectroscopy) depth profile

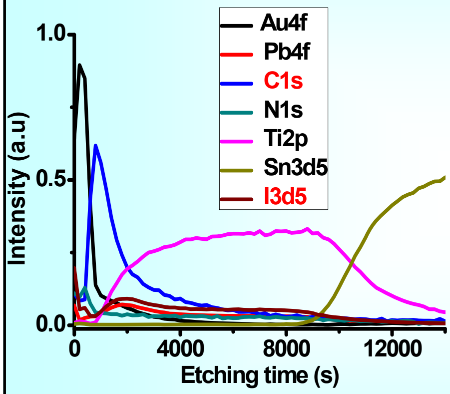

Photoluminescence (PL) spectra

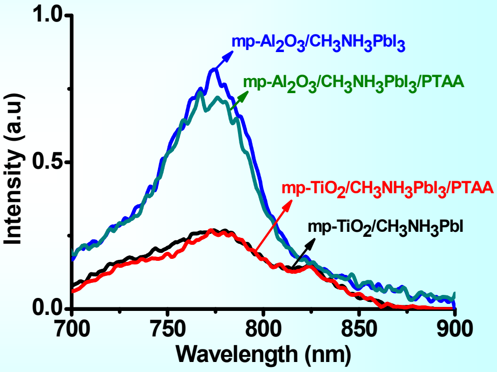

Nature Photonics, 7, 486–491 (2013)

Architectures

mp-TiO_2/CIS/C

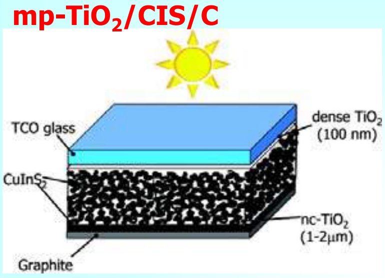

Table 1. EDX Results on Various Spots on the Sample Cross Section[a]

spect label	atomic % S (K)	atomic % Ti (K)	atomic % In (L)	atomic % Sn (L)
a				99.44
b	3.19		4.94	92.64
c	2.80	78.81	1.2	17.18
d	24.33	58.69	16.49	
e	67.87		32.1	

[a] Atomic concentration on specific spots is determined. The spot size for EDX measurements was 100 nm. The atomic ratio was calculated for sulfur, titanium, indium, and tin.

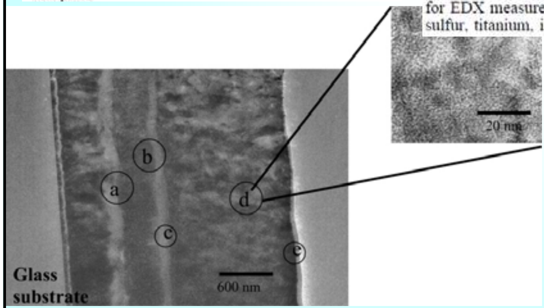

3D solar cells, with a remarkable energy conversion efficiency of 5%.

A. Goossens et al., Nano Lett., 5, 1716–1719 (2005)

Architectures

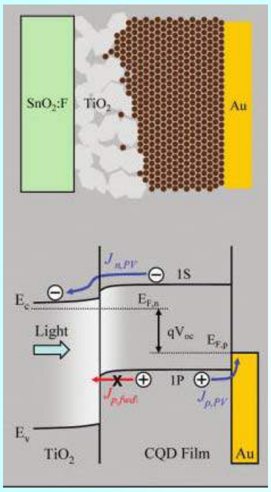

Depleted-Heterojunction Colloidal QD Cells

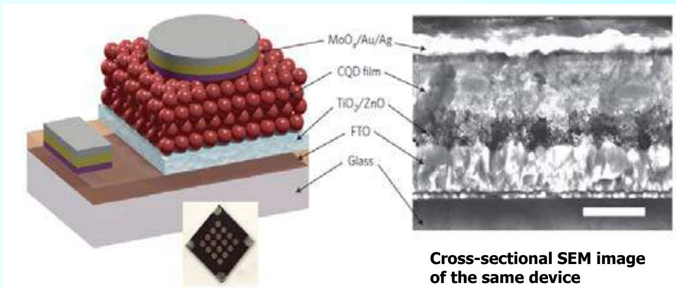

Schematic of the depleted heterojunction CQD device

Cross-sectional SEM image of the same device

Sargent et al., Nature Nanotechnology, 7, 577-582 (2012)

Sargent et al., ACS Nano, 4, 3374–3380 (2010)

mp-TiO_2/CITSe/Au solar cells

CITSe→The Cu:In:Te:Se precursor ratio of 1:1:1:2 resulted in $Cu_{0.23}In_{0.36}Te_{0.19}Se_{0.22}$ alloy QDs

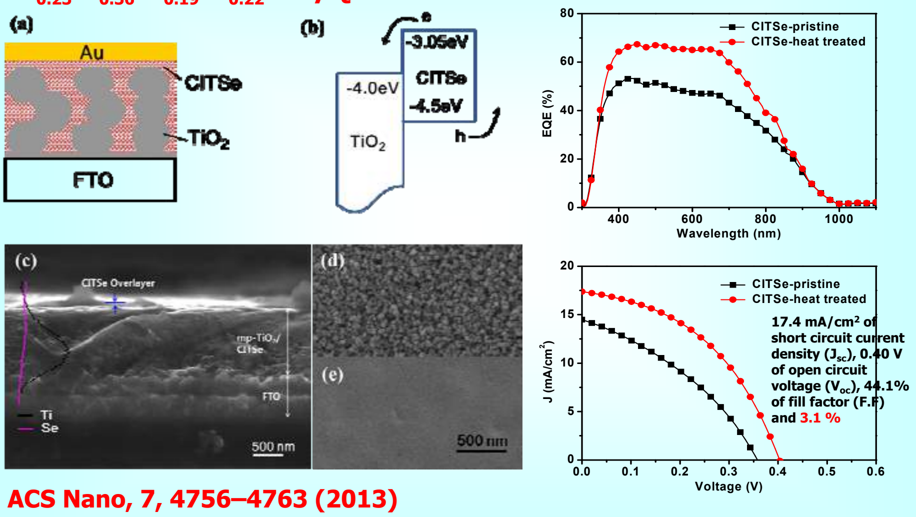

ACS Nano, 7, 4756–4763 (2013)

Architectures

mp-TiO_2/$MAPbI_3$/PTAA hybrid solar cells

3-D mp-TiO_2/perovskite nanocomposite and thin film layer]
→ pillared architecture, and new platform for efficient cells

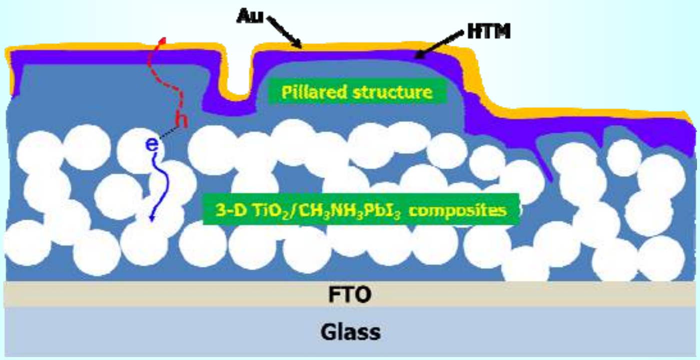

Nature Photonics, 7, 486 (2013)

Process for Bilayer architecture

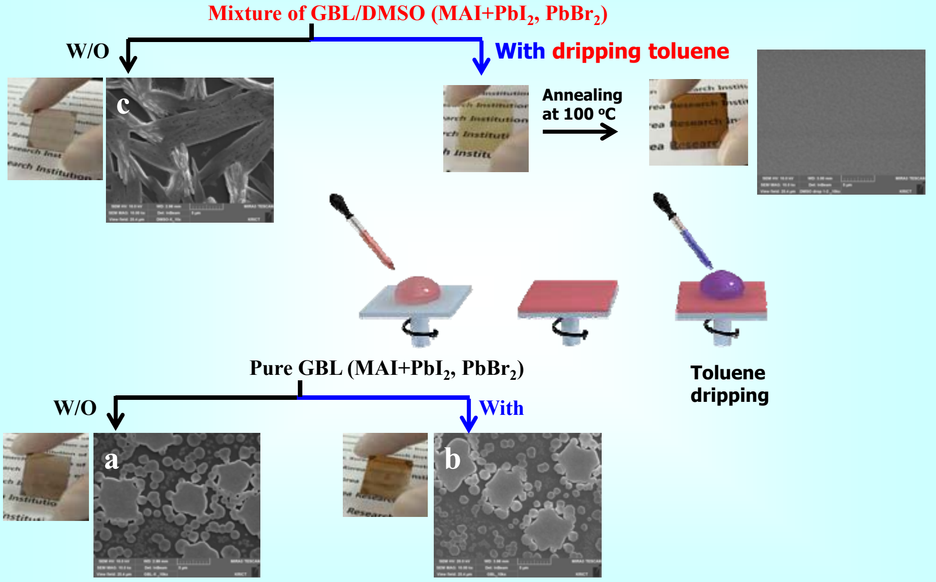

Process for Bilayer architecture

a, XRD spectra of PbI_2, MAI, $PbI_2(DMSO)_2$
b, FTIR spectrum of PbI_2-MAI-DMSO intermediate phase
c, XRD spectra of PbI_2-MAI-DMSO intermediate phase powder as a function of temperature

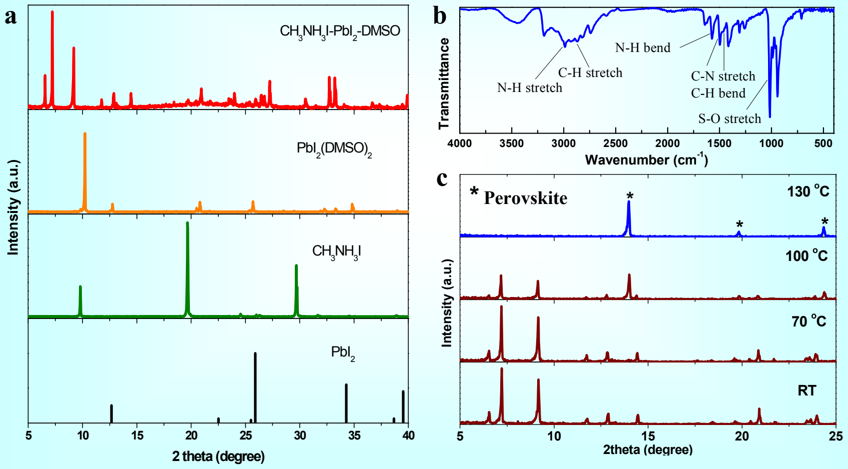

Process for Bilayer architecture

A plausible mechanism

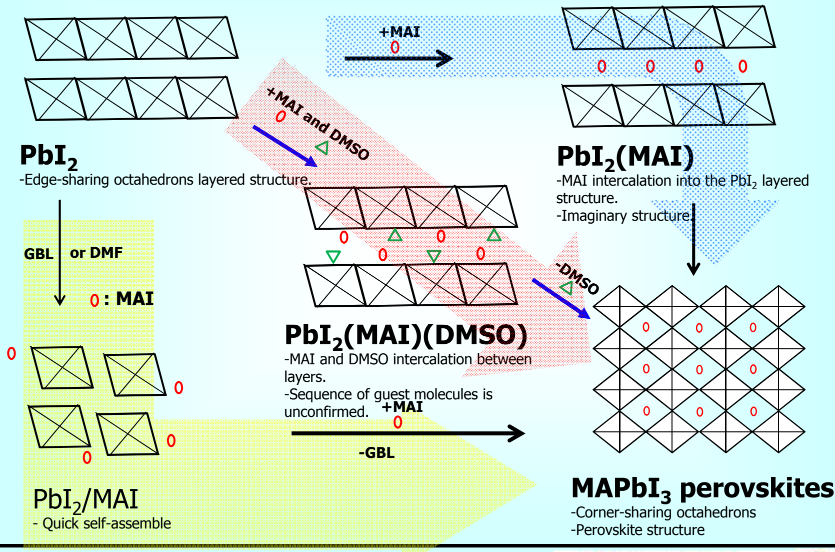

Nature Materials, 13 (2014) 897

Process for Bilayer architecture

H. J. Snaith et al., Nature, 501, 395 (2013)

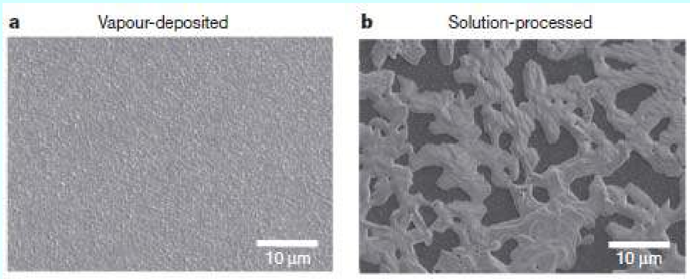

Solvent-engineering process

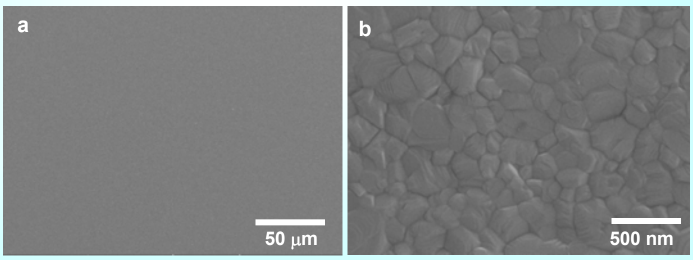

Efficient planar heterojunction perovskite solar cells by vapour deposition

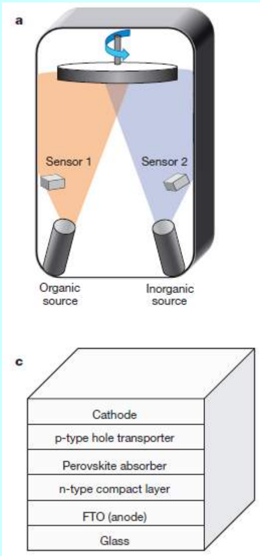

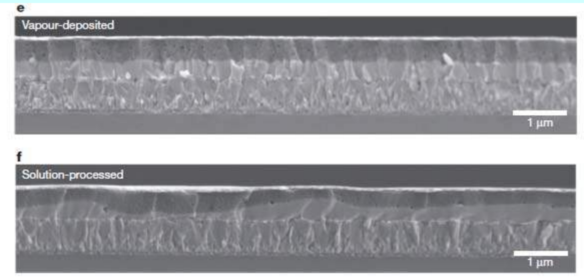

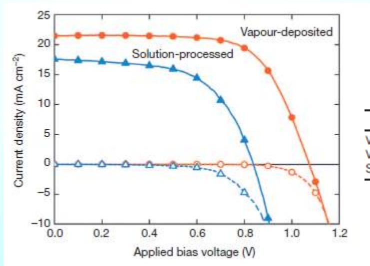

	Efficiency (%)
Vapour-deposited	15.4
Vapour-deposited (average ± s.d.)	12.3 ± 2.0
Solution-processed	8.6

H.J. Snaith et al., Nature, 2013, 501, 395–398

Hysteresis issue: Bilayer architecture

Photovoltaic performance as a function of scan direction and mp-TiO_2 thickness layer.

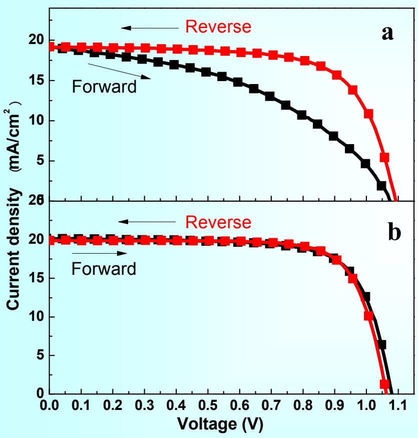

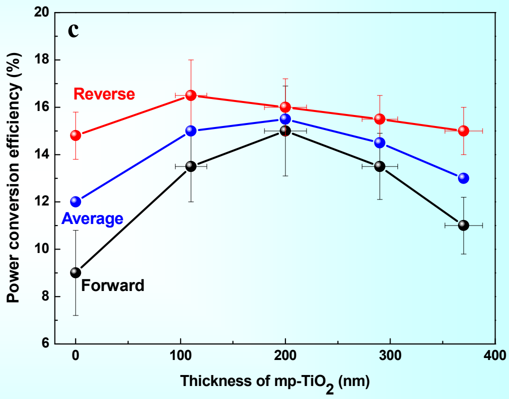

Nature Materials, 13 (2014) 897

Architecture: bilayer structure (balancing between e and h)

- P-I-N

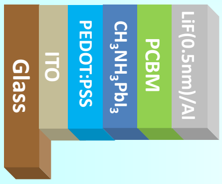

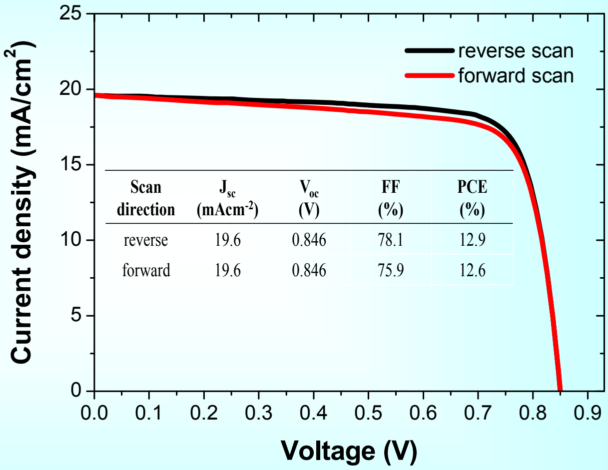

Scan direction	J_{sc} (mAcm^{-2})	V_{oc} (V)	FF (%)	PCE (%)
reverse	19.6	0.846	78.1	12.9
forward	19.6	0.846	75.9	12.6

- N-I-P
- Depletion thickness

Energy Environ. Sci., 2014, 7, 2642–2646

Materials: $CH_3NH_3Pb(I_{1-x}Br_x)_3$

Band-gap tuning ($MA=CH_3NH_3$)

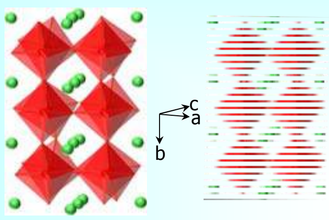

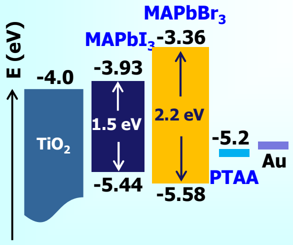

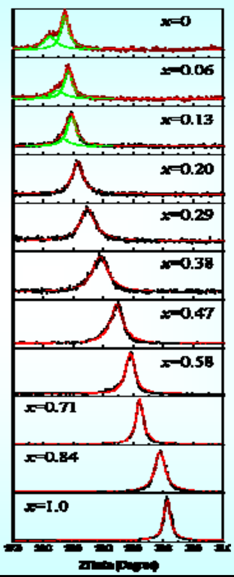

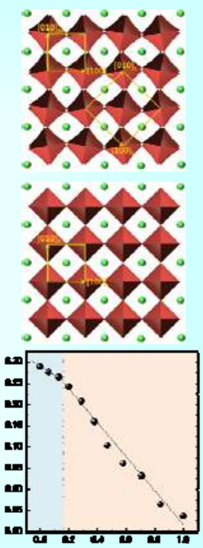

Nano Lett. 13, 1764–1769 (2013)

Materials: $CH_3NH_3Pb(I_{1-x}Br_x)_3$

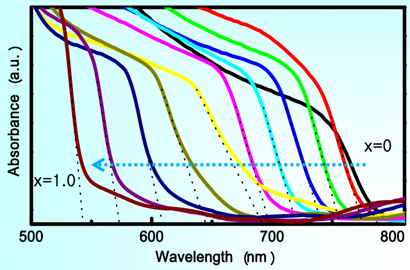

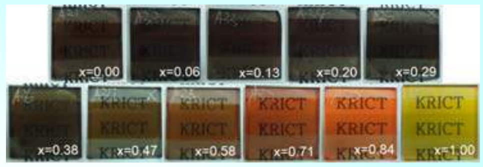

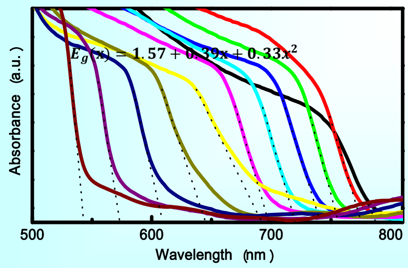

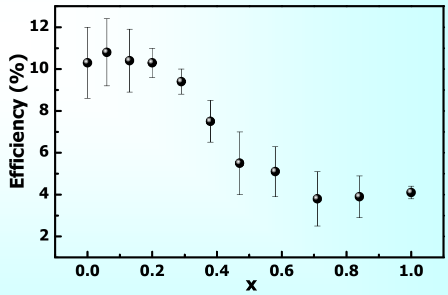

Nano Lett. 13, 1764–1769 (2013)

Materials: $CH_3NH_3Pb(I_{1-x}Br_x)_3$

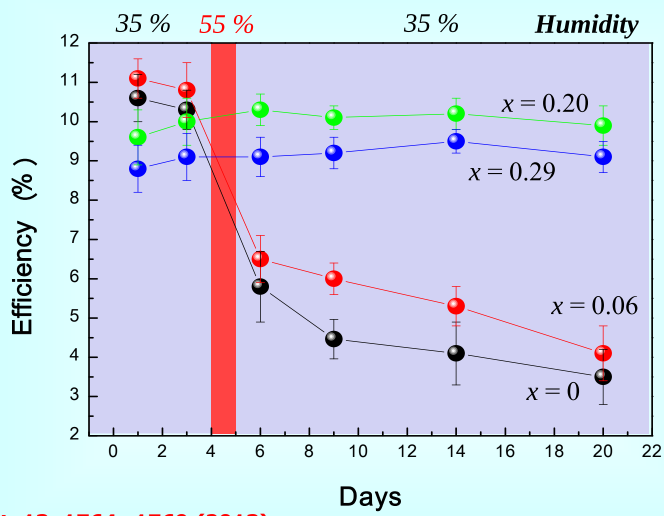

Nano Lett. 13, 1764–1769 (2013)

Materials: $CH_3NH_3Pb(I_{1-x}Br_x)_3$

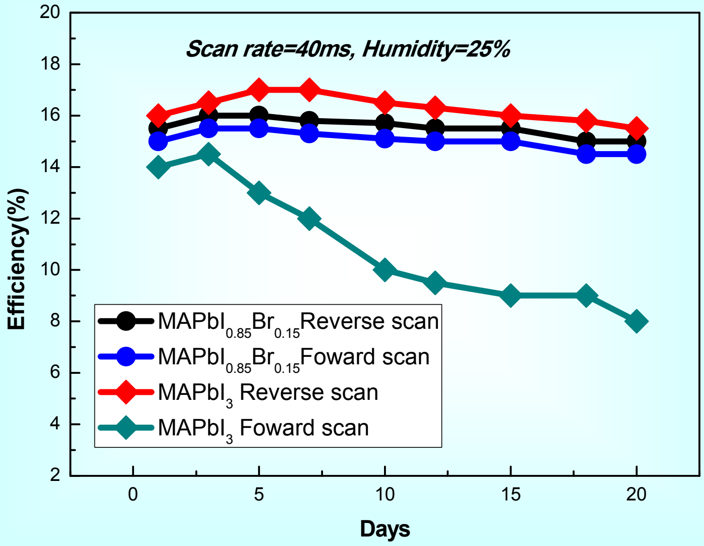

Materials: HTMs

spirobifluorene core in the spiro-OMeTAD→ Pyrene

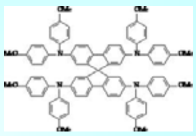

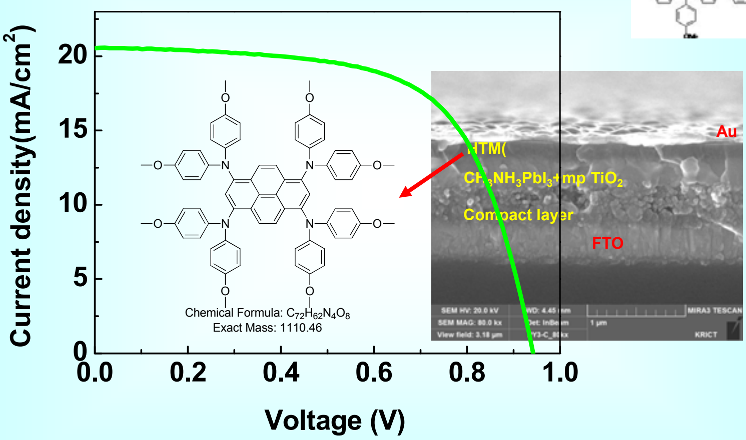

J. Am. Chem. Soc., 135, 19087 (2013)

Materials: HTMs

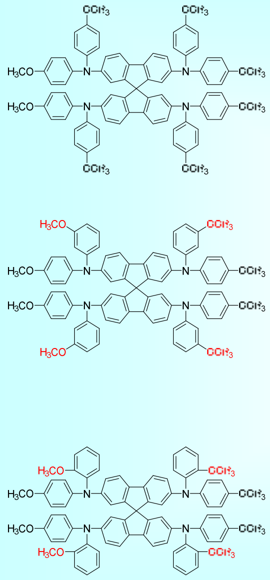

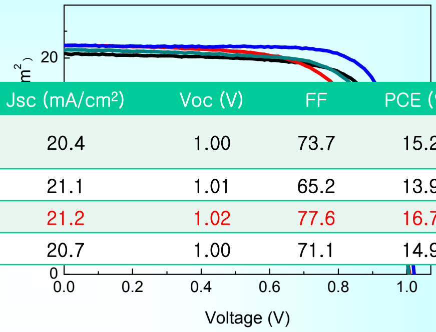

	Jsc (mA/cm²)	Voc (V)	FF	PCE (%)
merk(pp) Spiro	20.4	1.00	73.7	15.2
pm–Spiro	21.1	1.01	65.2	13.9
po–Spiro	21.2	1.02	77.6	16.7
pp–Spiro	20.7	1.00	71.1	14.9

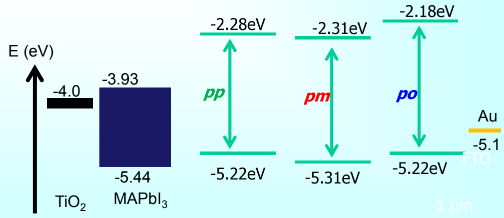

J. Am. Chem. Soc., 136, 7837 (2014)

KRICT Korea Research Institute of Chemical Technology

Materials: HTMs

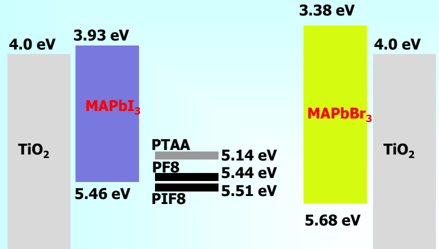

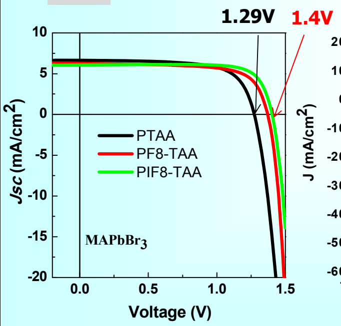

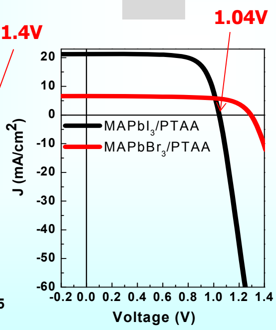

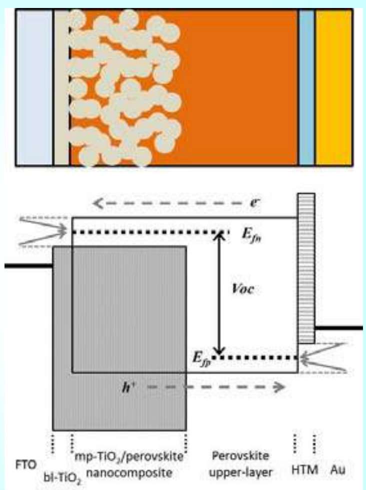

Energy & Environ Sci. 2014, 7, 2614–2618

KRICT Korea Research Institute of Chemical Technology

mp-TiO_2/$FAPbI_3$/PTAA hybrid solar cells

Materials: Phase stability

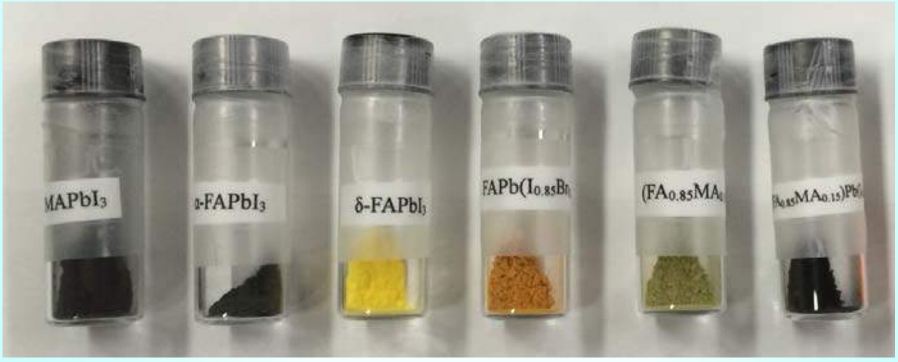

Photographs of inorganic-organic hybrid halide powders. Photographs show the color of the as-prepared $MAPbI_3$, annealed $FAPbI_3$ at 170 °C, $FAPbI_3$, $(FAPbI_3)_{1-x}(MAPbI_3)_x$, $(FAPbI_3)_{1-x}(FAPbBr_3)_x$, and $(FAPbI_3)_{1-x}(MAPbBr_3)_x$ powders with $x = 0.15$ (from left to right). The $(FAPbI_3)_{1-x}(MAPbBr_3)_x$ powder is the only black powder among the as-prepared $FAPbI_3$-based materials

mp-TiO_2/$FAPbI_3$/PTAA hybrid solar cells

Materials: Phase stability

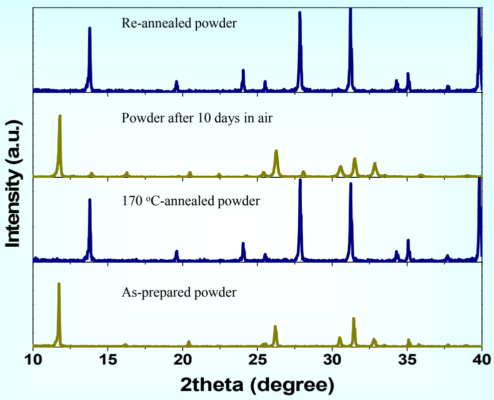

XRD spectra of $FAPbI_3$ powders. The as-prepared yellow $FAPbI_3$ powder shows a non-perovskite phase and is converted to perovskite phase by annealing at 170 °C. The perovskite $FAPbI_3$ black powder returned to the yellow non-perovskite powder after being stored in air for 10 h; the yellow powder reversibly changed to black perovskite phase by re-annealing at 170 °C.

mp-TiO_2/$FAPbI_3$/PTAA hybrid solar cells

Materials: Phase & morphology

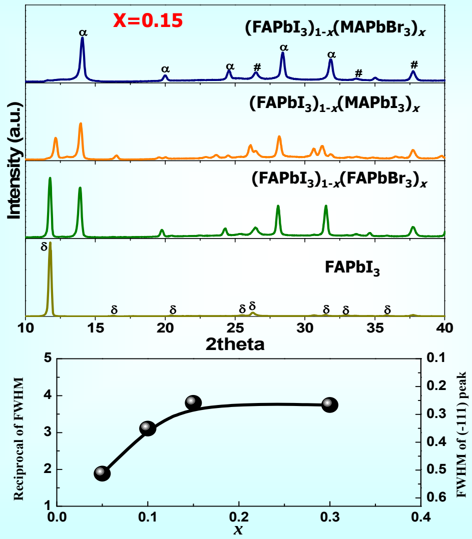

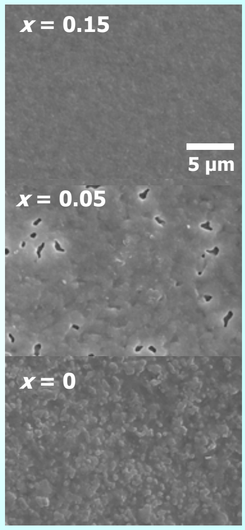

Nature, 517, 476–480 (2015)

mp-TiO_2/$(FAPbI_3)_{0.85}(MAPbBr_3)_{0.15}$/PTAA

Materials: $(FAPbI_3)_{1-x}(MAPbBr_3)_x$

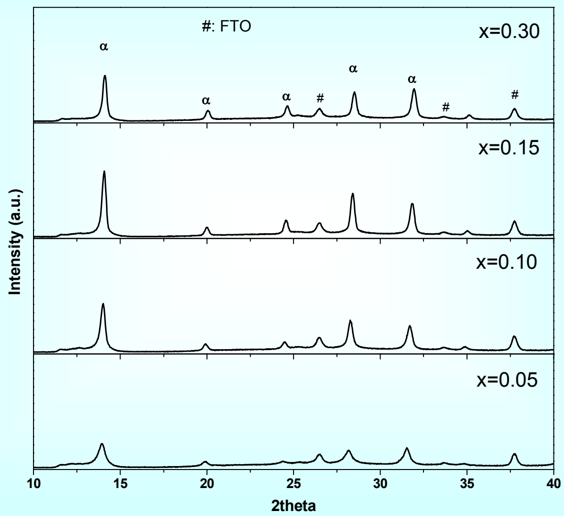

mp-TiO_2/$(FAPbI_3)_{0.85}(MAPbBr_3)_{0.15}$/PTAA

***J-V* and IPCE characteristics for the best cell obtained in $(FAPbI_3)_{0.85}(MAPbBr_3)_{0.15}$**

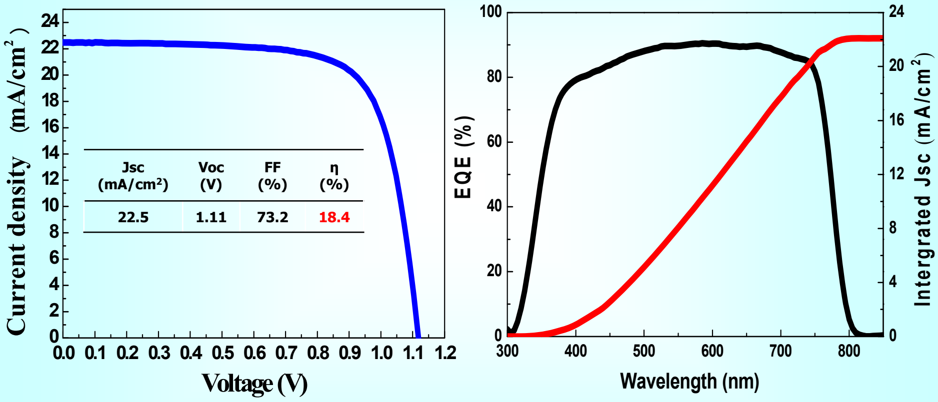

Nature, 517, 476–480 (2015)

Summary

- ✓ We sucessfully demonstrated efficient inorganic-organic hybrid solar cells antimony chalcogenides and perovskites as light harvesters.
- ✓ The hysteresis effect can be inhibited or even eliminated by using $FAPbI_3$ for N-I-P, and $MAPbI_3$ for P-I-N structure, respectively.
- ✓ The architecture, process, and composition for light harvesters should be optimized to fabricate further efficient solar cells